



Water balance modelling in a tropical watershed under deciduous forest (Mule Hole, India): Regolith matrix storage buffers the groundwater recharge process

Laurent Ruiz, M.R.R. Varma, M.S. Mohan Kumar, Muddu Sekhar, Jean-Christophe Maréchal, Marc Descloitres, Jean Riotte, Sat Kumar, C. Kumar, Jean-Jacques Braun

► To cite this version:

Laurent Ruiz, M.R.R. Varma, M.S. Mohan Kumar, Muddu Sekhar, Jean-Christophe Maréchal, et al.. Water balance modelling in a tropical watershed under deciduous forest (Mule Hole, India): Regolith matrix storage buffers the groundwater recharge process. *Journal of Hydrology*, 2010, 380 (3-4), pp.460-472. 10.1016/j.jhydrol.2009.11.020 . hal-00462049

HAL Id: hal-00462049

<https://hal.science/hal-00462049>

Submitted on 8 Mar 2010

HAL is a multi-disciplinary open access archive for the deposit and dissemination of scientific research documents, whether they are published or not. The documents may come from teaching and research institutions in France or abroad, or from public or private research centers.

L'archive ouverte pluridisciplinaire **HAL**, est destinée au dépôt et à la diffusion de documents scientifiques de niveau recherche, publiés ou non, émanant des établissements d'enseignement et de recherche français ou étrangers, des laboratoires publics ou privés.

**Water balance modelling in a tropical watershed under deciduous forest
(Mule Hole, India) : regolith matrix storage buffers the groundwater
recharge process**

Laurent Ruiz^{a,b,*}, Murari R. R. Varma^{c,d}, M. S. Mohan Kumar^{c,d}, M. Sekhar^{c,d}, Jean-
Christophe Maréchal^{c,e,f,g}, Marc Descloitres^{c,h}, Jean Riotte^{c,e,f,g} and Jean-Jacques Braun^{c,e,f,g}

^a INRA, UMR1069, Sol Agro et hydrosystème Spatialisation, 35000 Rennes, France

^b Agrocampus Ouest, UMR1069, Sol Agro et hydrosystème Spatialisation, 35000 Rennes,
France

^c Indo-French Cell for Water Sciences, IISc-IRD Joint laboratory, Indian Institute of Science,
560012 Bangalore, India

^d Indian Institute of Science, Department of Civil Engineering, , Bangalore 560 012, INDIA

^e Université de Toulouse ; UPS (OMP) ; LMTG; 14 Av Edouard Belin, F-31400 Toulouse,
France

^f CNRS ; LMTG ; F-31400 Toulouse, France

^g IRD ; LMTG ; F-31400 Toulouse, France

^h IRD ; Université de Grenoble ; CNRS ; LTHE , BP53, 38041 Grenoble, Cedex 9, France

* corresponding author:

Laurent RUIZ, INRA, Sol Agro and hydroSystemes, 4 rue Stang Vihan, F-29000 Quimper,
France

E-mail : ruiz@rennes.inra.fr

Tél : +33 (0) 2 98 95 99 64

Abstract

Accurate estimations of water balance are needed in semi-arid and sub-humid tropical regions, where water resources are scarce compared to water demand. Evapotranspiration plays a major role in this context, and the difficulty to quantify it precisely leads to major uncertainties in the groundwater recharge assessment, especially in forested catchments. In this paper, we propose a lumped conceptual model (COMFORT), which accounts for the water uptake by deep roots in the unsaturated regolith zone. The model is calibrated using a five year hydrological monitoring of an experimental watershed under dry deciduous forest in South India (Mule Hole watershed).

The model was able to simulate the stream discharge as well as the contrasted behaviour of groundwater table along the hillslope. Water balance simulated for a 32 year climatic time series displayed a large year-to-year variability, with alternance of dry and wet phases with a time period of approximately 14 years. On an average, input by the rainfall was 1090 mm.year⁻¹ and the evapotranspiration was about 900 mm.year⁻¹ out of which 100 mm.year⁻¹ was uptake from the deep saprolite horizons. The stream flow was 100 mm.year⁻¹ while the groundwater underflow was 80 mm.year⁻¹.

The simulation results suggest that i) deciduous trees can uptake a significant amount of water from the deep regolith, ii) this uptake, combined with the spatial variability of regolith depth, can account for the variable lag time between drainage events and groundwater rise observed for the different piezometers, iii) water table response to recharge is buffered due to the long vertical travel time through the deep vadose zone, which constitutes a major water reservoir.

This study stresses the importance of long term observatories for the understanding of hydrological processes in tropical forested ecosystems.

Key Words: matric porosity, groundwater recharge, lumped model, semi-arid tropics, evapotranspiration, vadose zone, forested watershed hydrology.

Introduction

Accurate assessment of water balance at the watershed scale is of major importance in a context of a global dramatic increase of human demand for water, either for urban or agricultural requirements. This assessment is complex, since water balance results from the interaction of climate, geology, morphology, soil and vegetation (De Vries and Simmers, 2002).

A large suit of rainfall-runoff models are available that are either fully empirical or mechanistic, which make it possible to predict with reasonable accuracy water balance from watersheds in temperate climates (Beven, 2001 ; Wagener et al., 2004). These models are usually evaluated according to their ability to simulate stream discharge. In semi-arid or arid climates, calibration of watershed models is difficult because streams are often ephemeral. Moreover, as potential evapotranspiration equals or surpasses average precipitation, a correct evaluation of actual evapotranspiration becomes crucial (Scanlon et al., 2002, 2006 ; Sekhar et al., 2004 ; Anuraga et al., 2006). Despite the large amount of work dedicated to assess evapotranspiration at the watershed scale, this flux remains the largest source of uncertainty in water budgeting, especially in the case of forested watersheds (Zhang et al., 2001; 2004).

The objective of this paper is to propose a methodology for water balance estimation in a tropical forested watershed, based on the calibration of a conceptual model against stream discharge and groundwater level data. The experimental watershed used in this study was developed as part of the project “Observatoire de Recherche en Environnement – Bassin Versant Expérimentaux Tropicaux” (<http://www.ore.fr/>) (Braun et al., 2005). Our results show that the deep vadose zone plays a major role in buffering the groundwater response to the water percolation.

Site description

The study site is situated in South India (Figure 1), at 11° 44' N and 76° 27' E (Karnataka state, Chamrajnagar district).

Figure 1: Location map of the experimental site

It is located in the transition zone of a steep climatic and geomorphologic gradient at the edge of the rifted continental passive margin of the Karnataka Plateau, which was the focus of extensive geomorphologic studies (Gunnell and Bourgeon, 1997). This plateau, developed on the high-grade metamorphic silicate rocks of the West Dharwar craton (Moyen et al., 2001), is limited westward by the Western Ghâts, a first order mountain range. This mountain forms an orographic barrier, inducing an steep climatic gradient, with annual rainfall decreasing from west to east from about 6000 mm to 500 mm within a distance of about 80 km (Pascal, 1982). These Ghâts are of critical ecological and economical importance and also an important source of all major South Indian rivers, flowing eastward towards the Gulf of Bengal. The climatic transition zone is mainly covered by dry deciduous forests, belonging to

the wildlife sanctuaries of Mudumalai, Waynad, Bandipur and Nagarahole (Prasad and Hedge, 1986). Such a tropical climosequence is comparable, although much steeper (Gunnell, 2000), to the well documented monsoonal West African and the Northeast Brazilian climosequences (Gunnell, 1998).

The Mule Hole experimental watershed (4.1 km²) is located in the climatic semi-humid transition area and the mean annual rainfall (n = 25 years) is 1120 mm. The mean yearly temperature is 27 °C. On the basis of the aridity index defined as the ratio of mean annual precipitation to potential evapotranspiration, the climate regime can be classified as humid (UNESCO, 1979). Nevertheless, the climate is characterized by the occurrence of a marked dry season (around 5 months from December to April) and by recurrent droughts, depending on the monsoon rainfalls. The rainfall pattern is bimodal, as it is affected by both the South West Monsoon (June to September) and the North East Monsoon (October - December) (Gunnell and Bourgeon, 1997). Streams are ephemeral, and their flow duration ranges from a few hours to a few days after the storm events.

The watershed is mostly undulating with gentle slopes and the elevation of the watershed ranges from 820 to 910 m above sea level (Figure 1). The morphology of the watershed is convexo-concave highly incised by the temporary stream network. The lithology, representative of the West Dharwar craton (Naqvi and Rogers, 1987), is dominated by complexly folded, heterogeneous Precambrian peninsular gneiss intermingled with mafic and ultramafic rocks of the volcano-sedimentary Sargur series (Shadakshara Swamy et al., 1995). The Peninsular gneiss represents at least 85% of the watershed basement and the average strike value is N80°, with a dip angle ranging from 75° to the vertical (Descloitres et al., 2008). In such hard-rock context, the aquifer can generally be divided into two parts: one

upper part is the porous clayey to loamy regolith with an apparent density lower than the rock bulk density, the other is in the fractured-fissured protolith with an apparent density close to the bulk density of the rock and a network of fractures of a density decreasing with depth (Sekhar et al., 1994, Maréchal et al., 2004 ; Wyna et al., 2004 ; Dewandel et al., 2006). In the Mule Hole watershed, the average depth of the regolith is 17 m, as estimated through an extensive geophysical and geochemical survey (Braun et al., 2006 ; Braun et al., 2008). The distribution of the regolith depth (Figure 2) shows that the range of variation is 5 to 27 m. No correlation with the position on the hillslope was found. Average total porosity of the regolith is around 12%. Magnetic Resonance Sounding (MRS) performed on the watershed (Legchenko et al., 2006) showed that drainage porosity is around 1% in the regolith and below the detection level ($<0.5\%$) in the fractured rock. Finally, timelapse geophysical measurements of both ERT and MRS conducted at the outlet of the watershed indicated a seasonal infiltration of water under the stream (Descloitres et al., 2008). A hydrological investigations allowed estimating the indirect recharge from the stream at around 30 mm.year⁻¹ at the watershed scale (Maréchal et al., 2009).

Figure 2 : distribution of regolith depth across the Mule Hole watershed (from a geophysical and geochemical survey by Braun et al., 2008)

The soil distribution in the watershed was determined by Barbiéro et al. (2007). The gneissic saprolite, cohesive to loose sandy, crops out both in the streambed and at the mid-slope in approximately 22% of the watershed area. The lower part of the slope and the flat valley bottoms (12% of the area) are covered by black soils (Vertisols and Vertic intergrades), which are 2 m deep on an average. Shallow red soils (Ferralsols and Chromic Luvisols), which are of 1 to 2 m deep, cover 66% of the entire watershed area. The watershed is covered by a dry

deciduous forest with different facies linked to the soil distribution (Barbiéro et al., 2007). Minimal human activity is present as it belongs to the Bandipur National Park, dedicated to wildlife and biodiversity preservation. The predominant tree component of the vegetation consists of *Anogeissus-Terminalia-Tectona* association (ATT facies) forming a relatively open canopy not exceeding 20 m (Prasad and Hedge, 1986 ; Pascal, 1986). Phenology is marked by a strong seasonality, with leaf senescence starting in December and leaf flushing occurring in early April, one or two month before the first significant monsoon rains. This surprising behaviour, leading to a deciduous period of only 2-3 months, much shorter than the dry season, is a general feature of the Asian forests (Singh and Kushawaha, 2005), and was quoted as the “paradox of Asian monsoon forest” by Elliot et al. (2006).

Model description

The model COMFORT (**CO**nceptual **M**odel for hydrological balance in **FOR**ested catchments) proposed in this article allows simulating the daily water budget of a forested watershed, through a simple and widely accepted conceptual description of the hydrological processes. It includes a lumped model for the soil moisture and the evapotranspiration in the forest (Granier et al., 1999), a surface runoff model based on the variable source area theory (Moore et al., 1983 ; Beven, 2001) and linear reservoirs for the recharge and groundwater discharge (Beven, 2001 ; Putty and Prasad, 2000). Its originality relies on the introduction of an additional water reservoir located in the weathered vadose zone (saprolite) below the soil, accessible to tree roots but not to understorey vegetation roots.

Figure 3 : A schematic representation of the model COMFORT

The model includes two modules, calibrated and run successively (Figure 3): the first one is a slightly modified and simplified version of the lumped water balance model presented by Granier et al (1999), which simulates the daily water balance for the forested soil and the surface runoff Q_s , while the second one simulates the flow of water through the deep vadose zone and the groundwater flow. Forcing variables are the daily rainfall (Rf), the Penman potential evapotranspiration (PET), and the forest leaf area index (LAI). The details of each of these modules is given below.

Module 1: Soil moisture

This module computes the daily variations in the soil moisture deficit (SMD, in mm) as:

$$\Delta SMD = E_{In} + T + E_u + PR + Q_s - Rf$$

and

$$0 < SMD < SMD_{max}$$

with E_{In} (mm.day^{-1}) being the evaporation of rainfall intercepted by the forest canopy, T (mm.day^{-1}) the tree transpiration, E_u (mm.day^{-1}) the evapotranspiration of the understorey layer, PR (mm.day^{-1}) is the percolation below the soil layer, also called “potential recharge” by De Vries and Simmers (2002), Q_s (mm.day^{-1}) the surface runoff, Rf (mm.day^{-1}) the rainfall and SMD_{max} (mm) the maximum soil water deficit, equivalent to the soil water holding capacity.

The throughfall ($R_f - E_{In}$) on the saturated area of the watershed (SA in %) reaches the stream as surface runoff (Q_s in mm.day^{-1}) :

$$Q_s = (R_f - E_{In}) \times SA / 100$$

Saturated area is usually computed as a function of water storage in the soil and the groundwater (see for example Putty and Prasad, 2000). In our context, groundwater level is far below the ground level, thus SA is modelled as an exponential function of the soil moisture deficit:

$$SA = SA_{\max} \times \exp(-a \times SMD)$$

with SA_{\max} the maximal extension of the saturated area (%), and a being the exponent constant. The proportion (%) of the soil surface covered by tree leaves (ϵ) is calculated from the forest LAI with the Beer-Lambert function assuming a light coefficient of extinction of 0.5 (Granier et al. 1999).

$$\epsilon = 1 - e^{-0.5 \times LAI}$$

The evaporation of rainfall intercepted by the forest canopy, or interception losses, E_{In} (mm.day^{-1}) is computed as:

$$E_{In} = \text{minimum}(\epsilon \times R_f ; \epsilon \times PET ; \epsilon \times I_n)$$

with I_n (mm) the canopy storage capacity. This equation implies that canopy cannot store water for more than one day, and thus interception losses are nil during non rainy days. This simplification is justified by the fact that I_n is generally smaller than PET at a daily time step.

As proposed by Granier et al. (1999), to account for the fact that the rate of evaporation of intercepted water is approximately four time greater than transpiration rate (Rutter, 1967), PET is reduced by 20 % of the amount of intercepted water and the total actual evapotranspiration (AET) is limited to $1.2 \times PET$. The tree transpiration from the soil layer (T_s in mm.day^{-1}) is then calculated as:

$$T_s = \text{minimum} (SMD_{\max} - SMD ; (\epsilon \times PET) - (0,2 \times E_{In}) ; 1.2 \times PET - E_{In})$$

with SMD_{\max} the maximum soil water deficit (mm), equivalent to the soil water holding capacity. In their model, Granier et al. (1999) propose that T/PET ratio decreases linearly when soil moisture reaches a critical level of 40% of the water holding capacity of the soil. In our model, for the sake of simplicity, transpiration is only limited by the amount of water present in the soil reservoir.

Evapotranspiration from understorey vegetation is calculated as:

$$E_u = \text{minimum} (SMD_{\max} - SMD - T_s ; (1-\epsilon) \times PET ; 1.2 \times PET - T_s - E_{In})$$

Actual evapotranspiration from the soil layer (AETs in mm.day^{-1}) is then:

$$AET_s = E_{In} + T_s + E_u$$

248

249 Eventually, the water in excess in the soil reservoir (when $SMD < 0$) percolates below the soil
250 layer, as “potential recharge” (PR in $mm.day^{-1}$). This flow is an input to the weathered zone
251 reservoir (module 2).

252

253 ***Module 2: Weathered zone and groundwater***

254

255 This module simulates the daily variations of the moisture deficit in the weathered zone
256 ($WZMD$ in mm) as :

257

$$258 \Delta WZMD = T_{WZ} + R - PR$$

259

260 where T_{WZ} is the tree transpiration from the weathered zone below the soil ($mm.day^{-1}$), PR the
261 potential recharge calculated in the module 1 ($mm.day^{-1}$) and R ($mm.day^{-1}$) the recharge. The
262 potential evapotranspiration from the weathered zone ($mm.day^{-1}$) is the residual of the
263 potential transpiration of trees minus the actual tree transpiration in the soil zone:

264

$$265 PET_{WZ} = \varepsilon \times PET - (0,2 \times E_{In}) - T_s$$

266

267 The actual transpiration from the weathered zone T_{WZ} ($mm.day^{-1}$) is then:

268

$$269 T_{WZ} = \text{minimum} (WZMD_{\max} - WZMD ; PET_{WZ})$$

270

271 with $WZMD_{\max}$ (mm) the maximum water deficit of the weathered zone.

272 Recharge (R_{WZ} in mm.day^{-1}) is the water in excess in the weathered zone (when $WZMD < 0$).

273 To account for the observed smoothness of the recharge process, R_{WZ} is directed to a recharge

274 reservoir R (mm), and the effective recharge (R_{GW} in mm.day^{-1}) reaching the groundwater

275 reservoir (GW in mm) is calculated as :

276

277
$$R_{GW} = \alpha_1 \times R$$

278

279 with α_1 (day^{-1}) the recession coefficient of the recharge reservoir R .

280

281 Eventually, the daily variation of water content in the groundwater reservoir (GW in mm) is

282 calculated as:

283

284
$$\Delta GW = R_{GW} - Q_{GW}$$

285

286 with the Q_{GW} the groundwater flow (mm.day^{-1}) calculated as :

287

288
$$Q_{GW} = \alpha_2 \times GW$$

289

290 with α_2 (day^{-1}) the recession coefficient of the groundwater reservoir GW . As the groundwater

291 level is always deeper than the stream bed at the outlet, this flow is considered as an

292 underflow.

293

294 The groundwater table level (L_{GW} in meters above sea level) is then calculated as:

295

296
$$L_{GW} = L_0 + GW / (Sy \times 1000)$$

297

298 with L_0 (masl) the altitude of the base of the aquifer and S_y its specific yield.

299

300 **Data acquisition and model calibration procedure**

301

302 The climatic data (daily rainfall and PET) necessary to run the model were available for the
303 period 2003-2007 from the automatic weather station (CIMEL, type ENERCO 407 AVKP)
304 installed at the Mulehole forest check post, which is 1.5 km West to the watershed outlet
305 (Figure 1). Daily rainfall data were available at the same location from 1976 to 1995 from
306 Indian Meteorological Department. Daily rainfall data were also available from the
307 Ambalavayal weather station, located 20 km west of the study site, for the years 1979 to
308 2004. As statistical analysis showed a strong correlation between the two stations, the seven
309 missing years (1996-2002) in the Mule Hole were inferred from the Ambalavayal data.
310 Granier et al. (1999) have shown that soil water content can be equally simulated in forest
311 stands under different climates either with models based on Penmann potential
312 evapotranspiration or with mechanistic approaches taking into account the canopy structure.
313 Although many studies have shown that evapotranspiration is greater from forest than for the
314 short size vegetation (Zhang et al., 2001) this difference is mainly attributed to better access
315 to soil water at depth. Thus Penmann potential evapotranspiration was used as a forcing
316 variable to the model.

317

318 As year to year variations in PET were little during the years 2003 to 2007, an average daily
319 PET series was calculated and applied to the period 1976-2002. Using an average annual
320 curve of PET does not affect much the rainfall-runoff models (Burnash, 1995 ; Oudin et al.,
321 2005). The simulations were run on the reconstructed time series 1976-2007. Stream

discharge (Q_s) is measured since August 2003 at a 6 minutes time step using a flume built at the outlet of the watershed. Due to technical problems, level recording was not available from 15th April 2007 to 7th August 2007. A set of 13 observation wells were drilled in the area in 2003 (P1-P6) and 2004 (P7-P13) (Figure 1). Most of these wells are dedicated to the monitoring of the effects of water seepage from the stream. Wells P2, P3, P5, P6, P9 and P10 are not influenced by the indirect recharge from the stream (Maréchal et al., 2009), and can be used to assess the direct recharge. The water levels are monitored in all the wells either manually at a monthly time step or automatically at an hourly time-step. Due to technical problems (among which elephant attacks), P2 and P9 didn't give reliable records and were not included in the analysis. Additional data from an observation well (OW9) monitored by the Department of Mines and Geology (Karnataka State) since 1975, and located 20 km east of the watershed, which is close to the forest border, was used in the analysis.

As no measurement of forest leaf surface were carried out in the watershed, the evolution of LAI was hypothesised from qualitative observations from the site and references from literature concerning local tree phenology (Prasad and Hedge, 1986 ; Sundarapandian et al., 2005) and NDVI records for Indian forests (Prasad et al., 2005). Seasonality of leaf flushing and senescence is mostly driven by photoperiod, and therefore can be taken as a constant from one year to the other (Elliot et al., 2006 ; Singh and Kushwaha, 2005). The proposed LAI pattern is presented in the Figure 4a along with ϵ variations. The comparison with the average monthly rainfall and PET over 32 years period (Figure 4b) shows that maximum PET is reached during the deciduous period and that on average, rainfall exceeds PET during five months.

Figure 4: a) daily forest LAI and coefficient of extinction ε , b) average monthly rainfall (Rf) (1976-2007) and PET (2003-2007). Vertical bars indicate standard deviation of Rf.

The two modules were run and calibrated successively, and the model performance was assessed using the Nash & Sutcliffe (1970) efficiency criterion. The module 1 is calibrated against the observed stream discharge values. This module has three forcing variables (Rf, PET and LAI) and four parameters (I_n , a , SA_{max} and SMD_{max}). As the sensitivity analysis showed that the model was little sensitive to I_n value, it was set at 1 mm and calibration was performed on the three remaining parameters. The time series obtained for the potential evapotranspiration from the weathered zone (PET_{wz}) and the potential recharge (PR) are then used as forcing variables for the module 2, which includes five parameters ($WZMD_{max}$, α_1 , α_2 , S_y and L_0). The module 2 is calibrated for each piezometer against observed water table levels. To minimize equivalence possibilities, the following procedure was adopted: because $WZMD_{max}$ determines the date of initial water table rise, it is first adjusted by trial and error; then the four remaining parameters are automatically calibrated, with S_y values constrained smaller than 0.01, according to the conclusions of MRS survey (Legchenko et al., 2006). For each calibration, the solver was run with contrasting sets of initial parameter values, which later converged towards the same solution.

Results

Figure 5: observed (black line) and simulated (grey line) daily surface runoff (Q_s in $mm.day^{-1}$) at the Mule Hole watershed outlet for the 5 years of monitoring. Secondary axis is daily rainfall (Rf) in mm.

The Figure 5 compares the observed and the simulated surface runoff (Q_s) at the Mule Hole watershed outlet for the 5 years of monitoring. The Nash-Sutcliffe parameter calculated using the monthly values is 74. Despite this relatively low value, the model was able to reproduce the general trend of observed runoff, in particular the delay between the first monsoon rains and the first observed stream runoff. On the other hand, it was unable to reproduce the runoff observed after summer storm events in 2005, because they are due to Hortonian flow, a mechanism that was not accounted for in the model. However, this kind of event is of marginal importance in this pedoclimatic context. Considering that rainfall is measured in only one weather station located outside the watershed and the high spatial variability of rainfall, especially during strong individual storms, a perfect fit was not expected. In particular in 2005, two events, on 22nd of October and 4th of November, produced 34 mm.day⁻¹ and 20 mm.day⁻¹ of runoff for rains of 52 mm.day⁻¹ and 28 mm.day⁻¹ respectively. For these events, the actual rainfall in the watershed was probably much higher than the measured one. This is likely to have affected the assessment of water balance for the year 2005, as these two storms represent about one quarter of the total yearly runoff. However, this kind of event remains very rare: during the five monitoring years, only these two events produced more than 20mm of runoff, and only five other individual events produced more than 10 mm of runoff.

The calibrated parameter values are: $a = 0.1$, $SA_{max} = 33.3\%$ and $SMD_{max} = 173$ mm. The value of maximal saturated area is probably overestimated, considering that the flat valley bottom overlaid by black soil occupies about 12% of the watershed area. The two exceptional storm events mentioned above played an important role in this overestimation. The calibrated value of SMD_{max} is consistent with the soil moisture monitoring carried out in 2004 and 2005

in the site, showing a maximum variation of volumetric water content of 7% in red and black soils (Barbiéro et al., 2007) and an average 2 m depth (Braun et al., 2006).

Table 1 : Soil water balance (mm.year⁻¹) for the monitored year and yearly average for the monitored period and the whole 32 year simulated period. Signification of terms is in the text. *2003-2006 average

Annual soil water balances as well as averages for the monitoring period and the 32 years simulation period are presented in the Table 1. Evapotranspiration is the most important sink for water, accounting for about 70% of rainfall. Interception is about 10% of rainfall, which is in the range of references values given in the literature for broad leaved forests (Ward and Robinson, 2000). Potential recharge is large (197 mm.year⁻¹ on the whole period), and displays an important year to year variability. It is larger than the estimate based on the regression equation proposed by Rangarajan and Athavale (2000) from tritium injection experiments in granitic areas in India, which gives a value of about 150 mm.year⁻¹ for the conditions of Mule Hole. This difference might be due to specificities of the study site, in particular the relatively low PET, mainly due to low temperatures linked with the altitude and to the forested environment which contributes to decrease soil compaction and increase infiltration potential (Bruijnzeel, 2004; Ilstedt et al., 2007). Results also show that the monitoring period is quite representative of the whole 32 years period with respect to the soil water balance.

Figure 6 : relative variation of water table level in hillslope piezometer, compared to simulated potential recharge. Reference values for water table depth are 16.8 m, 27.8 m, 39.1 m and 37.4 m for P10, P3, P5 and P6 respectively.

420

421 The Figure 6 compares the simulated daily potential recharge with observed relative
422 variations in the water table level in hillslope piezometers. Although all piezometers showed a
423 consistent global tendency to water level rise, they displayed significant contrasted behaviour.
424 The relatively shallow piezometer (P10) responded each year to recharge, and the water level
425 rise was almost simultaneous with the first occurrence of the potential recharge. Then the
426 water level variation pattern was smooth, and the yearly maximum level was reached each
427 year about two months after the end of the potential recharge period. For P3, the water table
428 level did not increase in 2004, however showed a steep increase at the end of the 2005 rainy
429 season, followed by a gentle continuous increase. In this well, ephemeral water table
430 variations suggest the occurrence of some preferential flow (from August to October in 2006
431 and 2007). Finally, the deep piezometers P5 and P6 displayed a declining tendency in 2004
432 and 2005, a stabilisation or a very gentle rise in 2006, and a marked rise at the end of the rainy
433 season 2007. These contrasted patterns of water table variation among the different hillslope
434 piezometers suggest that they are linked with local processes and not by a regional aquifer
435 dynamics.

436

437 ***Figure 7: Observed (dots) and simulated (lines) water level (in meter above sea level) in***
438 ***piezometer P3, P5 and P10 for the monitoring period.***

439

440 ***Table 2 : Model parameters for the 3 simulated piezometers.***

441

442 Comparison of the observed and the simulated water level variations in piezometers for the
443 monitoring period show a very good agreement (Figure 7), with Nash criteria values of 96.7,
444 94.1 and 95.0 for P10, P3 and P5 respectively. Calibrated parameters (Table 2) are relatively

similar for the three piezometers. The most contrasted parameter is $WZMD_{max}$, the maximum water deficit of the weathered zone, because it accounts for the observed very long lag-time between water table rise observed in P10 in comparison with P3 (more than one year) and with P5 (more than 3 years). The calibrated value of the specific yield is consistent with the values obtained in similar fractured rock context in the region (Sekhar et al. 2004 ; Sekhar and Ruiz, 2006 ; Maréchal et al., 2006).

The most surprising result is the small value of the recession coefficient of the recharge reservoir (α_1). The recharge flow reaching the groundwater table is then very smooth, and it is mostly compensated by the groundwater discharge. The consequence is that the variations in the water content of the deep vadose zone (regolith and recharge reservoirs) are very large, with a maximum range of variation for the entire 32 year period of 650 mm, 745 mm and 851 mm for P10, P3 and P5 respectively. Although very large, these variations are compatible with the material porosity, considering the depth of this vadose zone (from 15 m to 40 m).

Figure 8 : Simulated variations of water table level (in masl) in piezometer P3, P5 and P10 for the 32 year simulation period (lines). Dots represent observed values.

Table 3: Watershed balance components (in $mm \cdot year^{-1}$) for the piezometers P10, P3 and P5, for the monitoring period and the 32 year simulation and average watershed balance components calculated by weighted average (see text) .

Average water balances components for each piezometer during the monitoring period and the 32 years simulation period are presented in the Table 3. Unlike the observations for the soil water balance, the monitored period appears dryer than the entire period. This is due to

the fact that the effects of the drought period from 2001 to 2003 persist longer at depth, which is apparent from the late rising of the deepest piezometers. The simulated long term variations of piezometers (Figure 8) reveals an alternance of wet and dry phases, of 12-15 years duration period. Maximum level in P5 is reached 2 to 3 years later than in P10. This simulated pattern was compared to the data recorded by the Department of Mines and Geology (Karnataka State) from 1974 to 2007 in a shallow observation well located outside the forest zone 20 km east of the study site. Although at the annual scale the observation well is much more reactive than P10, they display a very similar long-term trend. This observation suggests that the model was able to describe reasonably the global long-term behaviour of the groundwater.

Figure 9 : Simulated variations of water table level (in masl) in piezometer P10 (black line, left Y-axis) and water level (depth to ground level in meters) recorded by Department of Mines and Geology from 1974 to 2007 in a shallow observation well located outside the forest zone 20 km east of the study site (grey line with dots, right Y-axis)

Figure 10 illustrates the simulated variations of evaporation and transpiration during two years. It shows that transpiration by trees from the soil layer is the dominant flux during most of the year, especially during rainy season. Soil evapotranspiration by the understorey vegetation can be significant during dry season, depending on the occurrence of isolated rainy events. Transpiration of water from the deep weathered zone occurs mainly during dry season, and during dry periods on the course of the monsoon season. Because the model computes transpiration successively from soil and then from the weathered zone, the latter can occur only when soil water is completely depleted, leading to abrupt alternances between the two fluxes (figure 10c), which are probably much smoother in reality.

Figure 10: Example of simulated daily evapotranspiration fluxes (in mm.day⁻¹) compared to PET during two years a) variations of LAI b) Ein and Eu c) Ts and Twz (see text for signification of abbreviations)

With an objective to obtain an assessment of the water balance at the watershed scale, we need to assess the representativity of the monitored piezometers with respect to the entire area. The parameter WZMD_{max}, which is driving the most important part of the observed piezometer variability, is probably linked with the regolith depth in the vicinity of the piezometer. P10 is located in an area where the regolith depth is around 8m, P3 around 15 m and P6 more than 20m. A resistivity logging performed on P5 suggested a regolith depth of 22m (Braun et al., 2008). As a first approach, we can consider that P10, P3 and P5 are representative of area with regolith depth of 0-12m, 12-18m and more than 18m respectively. According to the regolith depth distribution in the watershed (Figure 2), the proportion is 30%, 27% and 43% for P10, P3 and P5 respectively. With this hypothesis, the watershed balance (Table 3) appears roughly equilibrated during the 32 years simulation period, while the water gain was 125 mm.year⁻¹ during the monitoring period. The average water uptake by trees from the deep weathered zone is 104 mm, and average groundwater underflow is 78 mm.year⁻¹. Groundwater recharge is equivalent to underflow on the long term. This value is close to the recharge that was assessed in this area with Chloride mass balance method (45 mm.year⁻¹, Maréchal et al., 2009).

Discussion

The 5 years monitoring allowed us to give a tentative assessment of the water balance of a small experimental watershed using a simple conceptual lumped model. However, the

exercise has proven to be difficult, due to the climatic context and the presence of forest. The plausibility of the model results and the future work needed to validate them are discussed in this section.

One uncertainty is linked to the assessment of evapotranspiration in forest stands. This issue continues to generate a great deal of controversy in the literature (Andreassian, 2004 ; Bruijnzeel, 2004 ; Robinson et al., 2003). The difficulty is also greater for regions with the index of dryness (PET/Rf) close to 1.0 (Zhang et al., 2004), which is the case in our study site. However, despite its limitations, the Penman-Montieth PET approach has proven its ability to simulate soil water moisture in a broad range of climatic conditions and tree species (Granier et al., 1999). The average total evapotranspiration found in our long term simulations (around 900 mm.year⁻¹, out of which about 100 mm are linked to extra transpiration by deep tree roots, see Table 3) is in very good agreement with the worldwide evapotranspiration curve proposed for forests and grasslands by Zhang et al. (2001). In our climatic context, water percolation towards the deep vadose zone is mainly concentrated during short rainy periods of the monsoon season, usually few days to two weeks, followed by drier periods. In this configuration, soil water budget is less sensitive to evapotranspiration assessment. However, direct measurements of forest evapotranspiration would allow a better calibration of the model.

According to our model, the spatial variability of the water reservoir located at depth in the weathered zone and accessible to deep roots of trees is a key parameter for water budgeting in semi-arid forested watersheds. Our calibration gave values ranging from 50 to 470 mm (Table 2). Few studies have been dedicated to measure the hydraulic properties of weathered granitic rocks (Jones and Graham, 1993; Katsura et al., 2006). They suggest that weathered rocks have

the capacity to hold appreciable amount of water that is available to plants (Jones and Graham, 1993 ; Williamson et al., 2004). The fact that tree roots are able to uptake water at considerable depth, especially in water limited ecosystems is widely accepted (Nepstad et al., 1994 ; Canadell et al., 1996 ; Collins and Bras, 2007). Importance of water storage in deep weathered rock in forested ecosystems has recently gained recognition, and large scale surveys to quantify deep water reservoirs have been attempted, for example in Cambodia (Ohnuki et al., 2008), leading to estimates as high as 1350 mm. The average total porosity of the saprolite in the Mule Hole watershed was estimated at 12% from geophysical and geochemical studies (Braun et al., 2008). Even assuming that the proportion of the porosity available to plants is only 5%, considering a 16 m deep saprolite would lead to an average water storage capacity of 800 mm, which is compatible with our findings. Considerable spatial variability of water stress and tree mortality during drought period is commonly reported in dry deciduous forests (Nath et al., 2006). A survey dedicated to check whether part of this variability can be explained by the regolith depth would constitute a validation of our hypothesis.

The most surprising consequence of the model calibration is the great importance of the recharge reservoir, and its low recession coefficient. In temperate regions, recharge process is usually considered to be very quick, and in most models water percolated below the soil zone is immediately transferred to the groundwater. This is acceptable because groundwater table is generally shallow, and the regolith matric porosity is filled every year by recharge. However, the fact that matric water can drain for a long time is well documented (Healy and Cook, 2002). In a chalk aquifer, Price et al. (2000) demonstrated that the delay between recharge period and the smooth water table rise can be explained by matric water storage in the vadose zone, which is slowly released to groundwater during dry periods. By monitoring water

content variations in a 21m deep sandstone vadose zone, Rimon et al. (2007) found a variation of 660 mm of water content during a rainy season, and a slow decrease in water content during the dry season. In a hydrogeologic survey in Australia, in a granitic environment, Ghauri (2004) observes a long delay between rainfall and groundwater response, attributed to matrix storage in the deep vadose zone. If this hypothesis is confirmed, it could be of considerable importance for water resource evaluation in hard rock aquifers, because in most cases recharge is assessed through water table level methods (Healy and Cook, 2002). Monitoring of water content variations in the deep vadose zone of our experimental watershed would allow validating this hypothesis.

The modelled watershed balance leads to an average water flow of about $180 \text{ mm} \cdot \text{year}^{-1}$, out of which 80 mm is groundwater underflow. This underflow might reach the streams of higher order rivers, like Nugu Hole or Kabini (Figure 1). Indeed, it is very small compared to the estimates of the flows produced in the humid zone of the climatic gradient that range from 900 to $4700 \text{ mm} \cdot \text{year}^{-1}$ (Putty and Prasad, 2000). However, these high flows are produced during the rainy season, and during the dry season rivers virtually dry up (Putty and Prasad, 2000). Because groundwater underflow from transition area produces a fairly constant load, it might be of significant importance in sustaining the baseflow in large rivers during the dry season. This will be assessed through a regional modelling in a future work.

Conclusions

This study is based on a five years monitoring of an experimental forested watershed in the South India, and using a conceptual model of the water balance over a 32 years period allowed us to draw the following conclusions :

i) In tropical forest ecosystems, deciduous trees can uptake a significant amount of water from the deep regolith. This mechanism is particularly important at the end of the dry summer period, because the leaf flushing can precede monsoon rains by several weeks. More investigations are needed to check if variability in regolith depth can be linked to the variability of tree mortality during dry periods in monsoon season.

ii) This water uptake, combined with the spatial variability of regolith depth, can account for the variable lag time between drainage events and groundwater rise observed for the different piezometers.

iii) Water table response to the recharge is buffered due to the long vertical travel time through the deep vadose zone, which constitutes a major water reservoir. The five years monitoring period reveals that the watershed water balance is not equilibrated, mainly due to large variations in water content in the vadose zone. This observation is of great importance for water resource assessment, as water level fluctuation method is often used to estimate yearly groundwater recharge, especially in India (G.E.C., 1997). Our results show that this method can lead to an underestimation of recharge when vadose zone is large.

This study stresses the importance of long term observatories for the understanding of the hydrological processes in tropical forested ecosystems.

Acknowledgements

The Mule Hole basin is part of the ORE-BVET project (Observatoire de Recherche en Environnement – Bassin Versant Expérimentaux Tropicaux, www.orebvet.fr). Apart from the specific support from the French Institute of Research for Development (IRD), the Embassy of France in India and the Indian Institute of Science, our project benefited of funding from IRD and INSU/CNRS (Institut National des Sciences de l'Univers / Centre National de la

620 Recherche Scientifique) through the French programmes ECCO-PNRH (Ecosphère
621 Continentale: Processus et Modélisation – Programme National Recherche Hydrologique),
622 EC2CO (Ecosphère Continentale et Côtière) and ACI-Eau. It is also funded by the Indo-
623 French programme IFCPAR (Indo-French Center for the Promotion of Advanced Research
624 W-3000). The multidisciplinary research carried on the Mule Hole watershed began in 2002
625 under the control of the IFCWS (Indo-French Cell for Water Sciences), joint laboratory
626 IISc/IRD. We thank the Department of Mines and Geology of Karnataka for providing data
627 and the Karnataka Forest Department and the staff of the Bandipur National Park for all the
628 facilities and support they provided.

629

References

- Andréassian, V., 2004 Water and forests: from historical controversy to scientific debate. *Journal of Hydrology* 291, 1-27.
- Anuraga, T.S., Ruiz, L., Mohan Kumar, M.S., Sekhar, M. and Leijnse, T.A., 2006 Estimating groundwater recharge using land use and soil data: a case study in South India. *Agricultural Water Management* 84 (1-2) 65-76.
- Barbiéro, L., Parate, H. R., Descloitres, M., Bost, A., Furian, S., Mohan Kumar, M.S., Kumar, C., and Braun, J. J., 2007. Using a structural approach to identify relationships between soil and erosion in a semi-humid forested area, south india. *Catena* 70(3), 313–329.
- Beven, K.J., 2001. *Rainfall-runoff modelling: the primer*. Wiley, Chichester, 360p
- Braun J.J., Ruiz L., Riotte J., Mohan Kumar M.S., Murari V., Sekhar M., Barbiéro L., Descloitres M., Bost A., Dupré B., Lagane C., 2005. Chemical and physical weathering in the Kabini River Basin, South India. *Geochimica Cosmochimica Acta* 69 (10), A691-A691
- Braun, J.J., Descloitres, M., Riotte, J., Barbiéro, L., Fleury, S., Boeglin, J.L., Ruiz, L., Muddu, S., Mohan Kumar, M.S., Kumar, M.C., and Dupré, B., 2006. Regolith thickness inferred from geophysical and geochemical studies in a tropical watershed developed on gneissic basement: Moole Hole, Western Ghâts (South India). *Geochimica et Cosmochimica Acta* 70 (18), A65-A65
- Braun, J.J., Descloitres, M., Riotte, J., Fleury, S., Barbiéro, L., Boeglin, J.L., Violette, A., Lacarce, E., Ruiz, L., Sekhar, M., Mohan Kumar, M.S., Subramanian, S. and Dupré, B., 2008 Regolith mass balance inferred from combined mineralogical, geochemical and geophysical studies: Mule Hole gneissic watershed, South India. *Geochimica and Cosmochimica Acta*, <http://dx.doi.org/10.1016/j.gca.2008.11.013>

654 Bruijnzeel, L.A., 2004 Hydrological functions of tropical forests: not seeing the soil for the
655 trees? *Agriculture, Ecosystems & Environment*, 104(1), 185-228.

656 Burnash, R.J.C., 1995. In: V.P. Singh, Editor, *The NWS river forecast system—catchment*
657 *modeling*, Computer Models of Watershed Hydrology, Water Resources Publications,
658 Highlands ranch, Co. 311–366.

659 Canadell, J., Jackson, R.B., Ehleringer, J.R., Mooney, H.A., Sala, O.E., Schulze, E.-D., 1996.
660 Maximum rooting depth of vegetation types at the global scale. *Oecologia* 108, 583–595

661 Collins, D. B. G. and Bras, R. L., 2007. Plant rooting strategies in water-limited ecosystems.
662 *Water Resources Research* 43, W06407

663 Descloitres, M., Ruiz, L., Sekhar, M., Legchenko, A., Braun, J-J., Mohan Kumar, M. S., and
664 Subramanian, S., 2008. Characterization of seasonal local recharge using electrical
665 resistivity tomography and magnetic resonance sounding. *Hydrological Processes* 22(3),
666 384-394.

667 De Vries, J.J., and Simmers, I., 2002. Groundwater recharge: an overview of processes and
668 challenges. *Hydrogeology Journal* 10, 8–15.

669 Dewandel, B., Lachassagne, P., Wyns, R., Maréchal, J.C., Krishnamurthy, N.S., 2006. A
670 generalized 3-D geological and hydrogeological conceptual model of granite aquifers
671 controlled by single or multiphase weathering. *Journal of Hydrology* 330 (1-2): 260-284,
672 doi:10.1016/j.jhydrol.2006.03.026.

673 Elliot, S., Baker, P.J. and Borchert, R., 2006. Leaf flushing during the dry season : the
674 paradox of Asian monsoon forests. *Global ecology and biogeography* 15(3), 248-257.

675 G.E.C., 1997 *Groundwater Resource Estimation Methodology*. Report of the Groundwater
676 Resource Estimation Committee, Ministry of Water Resources, Government of India, New
677 Delhi, India, 100 pp

678 Ghauri, S. 2004 Groundwater trends in the Central Agricultural Region. Resource
679 Management Technical Report 269. Department of Agriculture, Western Australia. 66p.

680 Granier, A., Bréda, N., Biron, P. and Vilette, S., 1999. A lumped water balance model to
681 evaluate duration and intensity of drought constraints in forest stands. Ecological
682 Modelling 116, 269-283.

683 Gunnell, Y. and Bourgeon, G., 1997. Soils and climatic geomorphology on the Karnataka
684 plateau, peninsular India. CATENA 29, 239-262.

685 Gunnell, Y., 1998. Passive margin uplifts and their influence on climatic change and
686 weathering patterns of tropical shield regions. Global and Planetary Change 18(1-2), 47-
687 57.

688 Gunnell, Y., 2000. The characterization of steady state in Earth surface systems: findings
689 from the gradient modelling of an Indian climosequence. Geomorphology 35, 11-20.

690 Healy, R.W. and Cook, P.G., 2002. Using groundwater levels to estimate recharge.
691 Hydrogeology Journal 10(1) 91-109.

692 Ilstedt, U., Malmer, A., Verbeeten, E., Murdiyarso, D., 2007. The effect of afforestation on
693 water infiltration in the tropics: a systematic review and meta-analysis. Forest Ecology and
694 Management 251 (1–2), 45–51.

695 Jones, D.P. and Graham, R.C., 1993. Water-holding characteristics of weathered granitic rock
696 in chaparral and forest ecosystems. Soil Science Society of America Journal 57, 256-261.

697 Katsura, S., Kosugi, K., Yamamoto, N. and Mizuyama, T., 2006. Saturated and unsaturated
698 hydraulic conductivities and water retention characteristics of weathered granitic bedrock.
699 Vadose Zone Journal 5(1), 35-47.

700 Legchenko, A., Descloitres, M., Bost, A., Ruiz, L., Reddy, M., Girard, J. P., Sekhar, M.,
701 Mohan Kumar, M. S., and Braun, J.-J., 2006. Resolution of MRS applied to the
702 characterization of hard-rock aquifers. Ground Water 44, 547-554.

703 Maréchal, J. C., Dewandel, B. and Subrahmanyam, K., 2004. Use of hydraulic tests at
704 different scales to characterize fracture network properties in the weathered-fractured layer
705 of a hard rock aquifer. *Water Resources Research* 40, W11508.

706 Maréchal, J.C., Dewandel, B., Ahmed, S., Galeazzi, L., and Zaidi, F.K., 2006. Combined
707 estimation of specific yield and natural recharge in a semi-arid groundwater basin with
708 irrigated agriculture. *Journal of Hydrology* 329(1-2), 281-293.

709 Maréchal, J.C., Varma, M.R.R., Riotte, J., Vouillamoz, J.M., Mohan Kumar, M.S., Ruiz, L.,
710 Sekhar, M., Braun, J.J., 2009 Indirect and direct recharges in a tropical forested watershed:
711 Mule Hole, India. *Journal of Hydrology*, 364 (3-4), 272-284.

712 Moore, I.D., Coltharp, G.B. and Sloan, P.G., 1983. Predicting runoff from small Appalachian
713 watersheds. *Transactions of the Kentucky Academy of Sciences (USA)*, 44(3/4), 135-145

714 Moyen, J.F., Martin, H. and Jayananda, M., 2001. Multi-element geochemical modeling of
715 crust-mantle interactions during late-Archean crustal growth: the Closepet Granite (South
716 India). *Precambrian Research* 112 (1-2), 87-105.

717 Naqvi, S. M. and Rogers, J. W., 1987. *Precambrian geology of India*. Clarendon Press,
718 Oxford University Press, New york.

719 Nash, J. E. and Sutcliffe, J. V., 1970. River flow forecasting through conceptual models. Part
720 I. A discussion of principles. *Journal of Hydrology* 10 (3) 282–290.

721 Nath, C.D., Dattaraja, H.S., Suresh, H.S., Joshi, N.V. and Sukumar, R., 2006. Patterns of tree
722 growth in relation to environmental variability in the tropical dry deciduous forest at
723 Mudumalai, southern India. *Journal of Biosciences* 31, 651–669.

724 Nepstad, D.C., Carvalho, C.R., Davidson, E.A., Jipp, P., Lefebvre, P., Negreiros, G.H.d., da
725 Silva, E.D., Stone, T.A., Trumbore, S. and Vieira, S., 1994. The role of deep roots in the
726 hydrological and carbon cycles of Amazonian forests and pastures. *Nature* 372, 666–669.

727 Ohnuki, Y., Kimhean, C., Shinomiya, Y. and Toriyama, J., 2008. Distribution and
 728 characteristics of soil thickness and effects upon water storage in forested areas of
 729 Cambodia. *Hydrological Processes* 22, 1272-1280.

730 Oudin, L., Michel, C., and Anctil, F., 2005. Which potential evapotranspiration input for a
 731 lumped rainfall-runoff model? Part 1-Can rainfall-runoff models effectively handle
 732 detailed potential evapotranspiration inputs? *Journal of Hydrology* 303, 275–289.

733 Pascal, J.P., 1982. Forest map of South India, 1/250 000 scale, sheet Mercara–Mysore.
 734 Travaux Section Scientifique et Technique Institut Français de Pondichéry, hors série, vol.
 735 18a.

736 Pascal, J.P., 1986. Explanatory booklet on the forest map of South India. Travaux Section
 737 Scientifique et Technique Institut Français de Pondichéry, Hors Serie, vol. 18.

738 Prasad, V.K., Anuradha, E., Badinath, K.V.S., 2005. Climatic controls of vegetation vigor in
 739 four contrasting forest types of India-evaluating from National Oceanic and Atmospheric
 740 Administration's Advanced Very High Resolution Radiometer datasets (1990–2000).
 741 *International Journal of Biometeorology* 50, 6–16.

742 Prasad, S.N. and Hedge, M., 1986. Phenology and seasonality in the tropical deciduous forest
 743 of Bandipur, South India. *Proceedings of the Indian Academy of Sciences (Plant Sci.)*
 744 96(2), 121-133.

745 Price, M., Low, R. G., and McCann, C., 2000. Mechanisms of water storage and flow in the
 746 unsaturated zone of the Chalk aquifer. *Journal of Hydrology* 233(1-4), 54-71.

747 Putty, M.R.Y. and Prasad, R., 2000. Understanding runoff processes using a watershed model
 748 - a case study in the Western Ghats in South India. *Journal of Hydrology* 228, 215-227.

749 Rangarajan, R., and Athavale R.N., 2000. Annual replenishable ground water potential of
 750 India - an estimate based on injected tritium studies. *Journal of Hydrology*, 234(1-2), 38-
 751 53.

752 Rimón, Y., Dahan, O., Nativ, R. and Geyer S., 2007. Water percolation through the deep
753 vadose zone and groundwater recharge: Preliminary results based on a new vadose zone
754 monitoring system. *Water Resources Research* 43, W05402.

755 Robinson, M., Cognard-Plancq, A. -L., Cosandey, C., David, J., Durand, P., Fuhrer, H. -W.,
756 Hall, R., Hendriques, M. O., Marc, V., McCarthy, R., McDonnell, M., Martin, C., Nisbet,
757 T., O'Dea, P., Rodgers, M. and Zollner, A., 2003. Studies of the impact of forests on peak
758 flows and baseflows: a European perspective. *Forest Ecology and Management* 186(1-3),
759 85-97.

760 Rutter, A.J., 1967. An analysis of evaporation from a stand of Scots pine. In: Sopper, W.E.,
761 Lull, H.W. (Eds.), *Forest Hydrology*. Pergamon Press, Oxford.

762 Scanlon, B.R., Healy, R.W. and Cook, P.G., 2002 Choosing appropriate techniques for
763 quantifying groundwater recharge. *Hydrogeology Journal* 10(1) 18-39.

764 Scanlon, B.R., Keese, K.E., Flint, A.L., Flint, L.E., Gaye, C.B., Edmunds, W. M, and Simmers,
765 I., 2006. Global synthesis of groundwater recharge in semiarid and arid regions.
766 *Hydrological Processes* 20(15), 3335-3370.

767 Sekhar, M. and Ruiz, L., 2006. Regional Groundwater Modeling: A Case study of Gundal
768 sub-basin, Karnataka, India. In Krishnaswamy, J., Lele, S. and Jayakumar, R. (Eds.)
769 *Hydrology and Watershed Services in the Western Ghats of India: Effects of land use and*
770 *land cover change*. Tata-McGraw-Hill, New Delhi, India. 81-103.

771 Sekhar, M., Rasmi, S.N., Sivapullaia, P.V. and Ruiz, L., 2004. Groundwater flow modeling of
772 Gundal sub-basin in Kabini river basin, India. *Asian Journal of Water Environmental*
773 *Pollution* 1 (1-2), 65-77.

774 Sekhar, M., Mohan Kumar, M.S. and Sridharan, K., 1994. Parameter estimation in an
775 anisotropic leaky aquifer system. *Journal of Hydrology* 163, 373-391.

776 Shadakshara Swamy, N., Jayananda, M., and Janardhan, A. S., 1995. Geochemistry of
 777 Gundlupet gneisses, Southern Karnataka: a 2.5 Ga old reworked sialic crust. In: Yoshida,
 778 M., Santosh, M., and Rao, A. T. Eds.), India as a fragment of East Gondwana. Gondwana
 779 Research Group.

780 Singh, K.P. and Kushwaha, C.P., 2005. Emerging paradigms of tree phenology in dry tropics.
 781 Current Science 89(6) 964-975.

782 Sundarapandian, S.M., Chandrasekaran, S. and Swamy, P.S., 2005. Phenological behaviour of
 783 selected tree species in tropical forest at Kodayar in te Western Ghats, Tamil Nadu, India.
 784 Current Science 88(5) 805-810.

785 UNESCO, 1979. Map of the world distribution of arid regions, 54 pp, UNESCO, Paris.

786 Wagener, T., Wheeler H.S. and Gupta, H.V., 2004. Rainfall-runoff Modelling in Gauged and
 787 Ungauged Catchments. Imperial College Press, London, 300p

788 Ward, R.C. and Robinson, M., 2000. Principles of hydrology. McGraw-Hill, London (4th
 789 edition), 450p.

790 Williamson, T.N., Newman, B.D., Graham, R.C. and Shouse, P.J., 2004. Regolith water in
 791 zero-order chaparral and perennial grass watersheds four decades after vegetation
 792 conversion. Vadose Zone Journal 3(3),1007-1016.

793 Wyns, R., Baltassat, J.M., Lachassagne, P., Legchenko, A., Vairon, J. and Mathieu, F., 2004.
 794 Application of proton magnetic resonance soundings to groundwater reserve mapping in
 795 weathered basement rocks (Brittany, France). Bulletin de la Société Géologique de France
 796 175(1), 21-34.

797 Zhang, L., Dawes, W. R., and Walker, G. R., 2001. Response of mean annual
 798 evapotranspiration to vegetation changes at catchment scale. Water Resources Research
 799 37(3), 701–708.

800 Zhang, L., Hickel, K., Dawes, W. R., Chiew, F. H. S., Western, A. W. and Briggs, P. R.,
801 2004. A rational function approach for estimating mean annual evapotranspiration. Water
802 Resources Research 40, W02502, doi:10.1029/2003WR002710.

803 List of Figures:

804

805 Figure 1: Location map of the experimental site

806

807 Figure 2 : distribution of regolith depth across the Mule Hole watershed (from a geophysical
808 and geochemical survey by Braun et al., 2008)

809

810 Figure 3 : A schematic representation of the model COMFORT

811

812 Figure 4: a) daily forest LAI and coefficient of extinction ϵ , b) average monthly rainfall (Rf)
813 (1976-2007) and PET (2003-2007). Vertical bars indicate standard deviation of Rf.

814

815 Figure 5: observed (black line) and simulated (grey line) daily surface runoff (Q_s in mm.day^{-1})
816 ¹) at the Mule Hole watershed outlet for the 5 years of monitoring. Secondary axis is daily
817 rainfall (Rf) in mm.

818

819 Figure 6 : relative variation of water table level in hillslope piezometer, compared to
820 simulated potential recharge. Reference values for water table depth are 16.8 m, 27.8 m, 39.1
821 m and 37.4 m for P10, P3, P5 and P6 respectively.

822

823 Figure 7: observed (dots) and simulated (lines) water level (in meter above sea level) in
824 piezometer P3, P5 and P10 for the monitoring period.

825

826 Figure 8 : simulated variations of water table level (in masl) in piezometer P3, P5 and P10 for
827 the 32 year simulation period (lines). Dots represent observed values.

828

829 Figure 9 : simulated variations of water table level (in masl) in piezometer P10 (black line,
830 left Y-axis) and water level (depth to ground level in meters))recorded by Central
831 Groundwater Board from 1974 to 2007 in a shallow observation well located in an
832 agricultural zone 20 km east of the study site (grey line with dots, right Y-axis)

833

834 Figure 10: example of simulated daily evapotranspiration fluxes (in mm.day^{-1}) compared to
835 PET during two years a) variations of LAI ; b) E_{in} and E_u ; c) T_s and T_{wz} (see text for
836 signification of abbreviations)

837

838 List of tables :

839

840 Table 1 : Soil water balance (mm.year^{-1}) for the monitored year and yearly average for the
841 monitored period and the whole 32 year simulated period. Signification of terms is in the text.

842 *2003-2006 average

843

844 Table 2 : model parameters for the 3 simulated piezometers.

845

846 Table 3: watershed balance components (in mm.year^{-1}) for the piezometers P10, P3 and P5,
847 for the monitoring period and the 32 year simulation and average watershed balance
848 components calculated by weighted average (see text).

849

Figure 1
[Click here to download high resolution image](#)

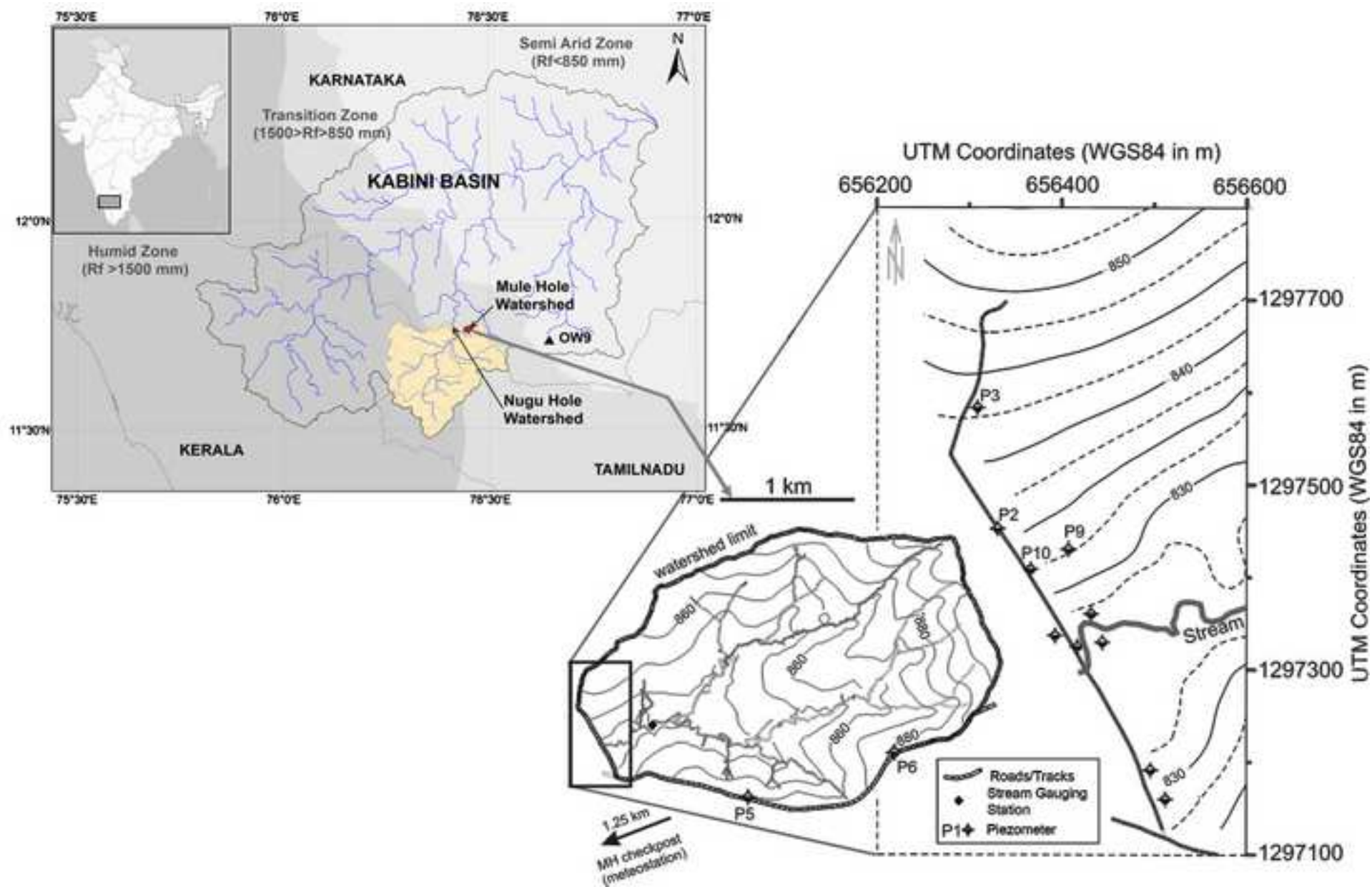


Figure 2
[Click here to download high resolution image](#)

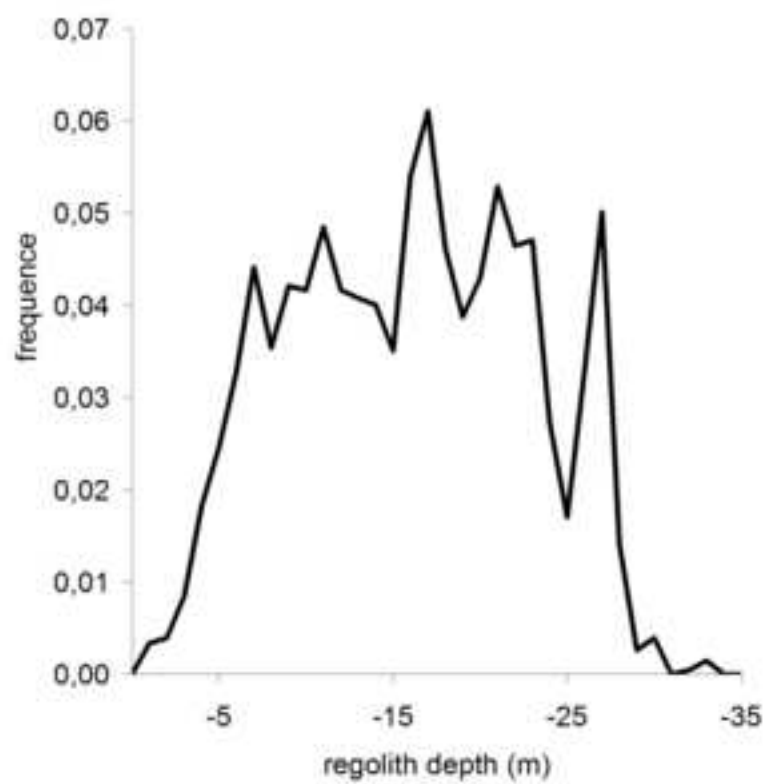


Figure 3
[Click here to download high resolution image](#)

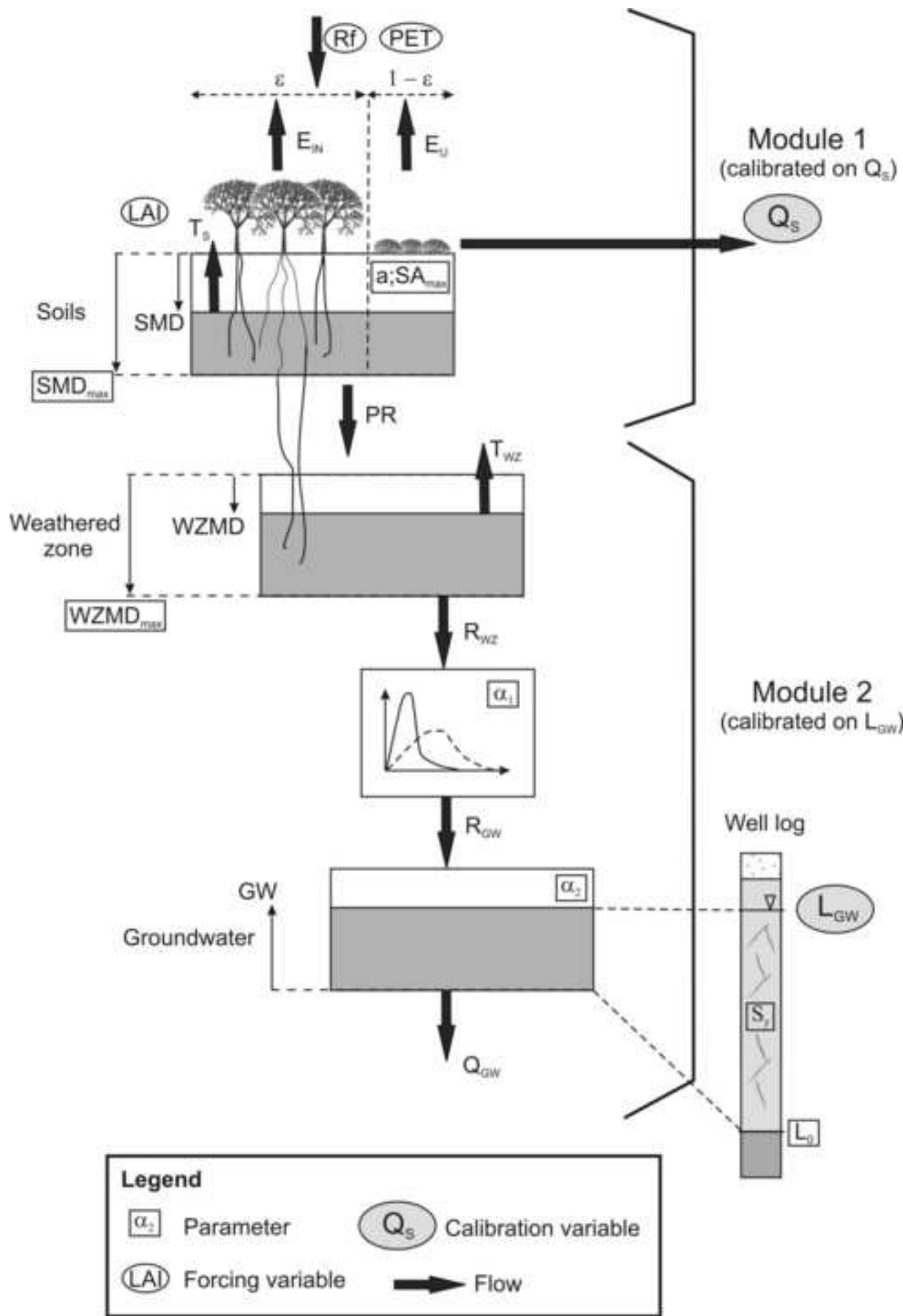


Figure 4

[Click here to download high resolution image](#)

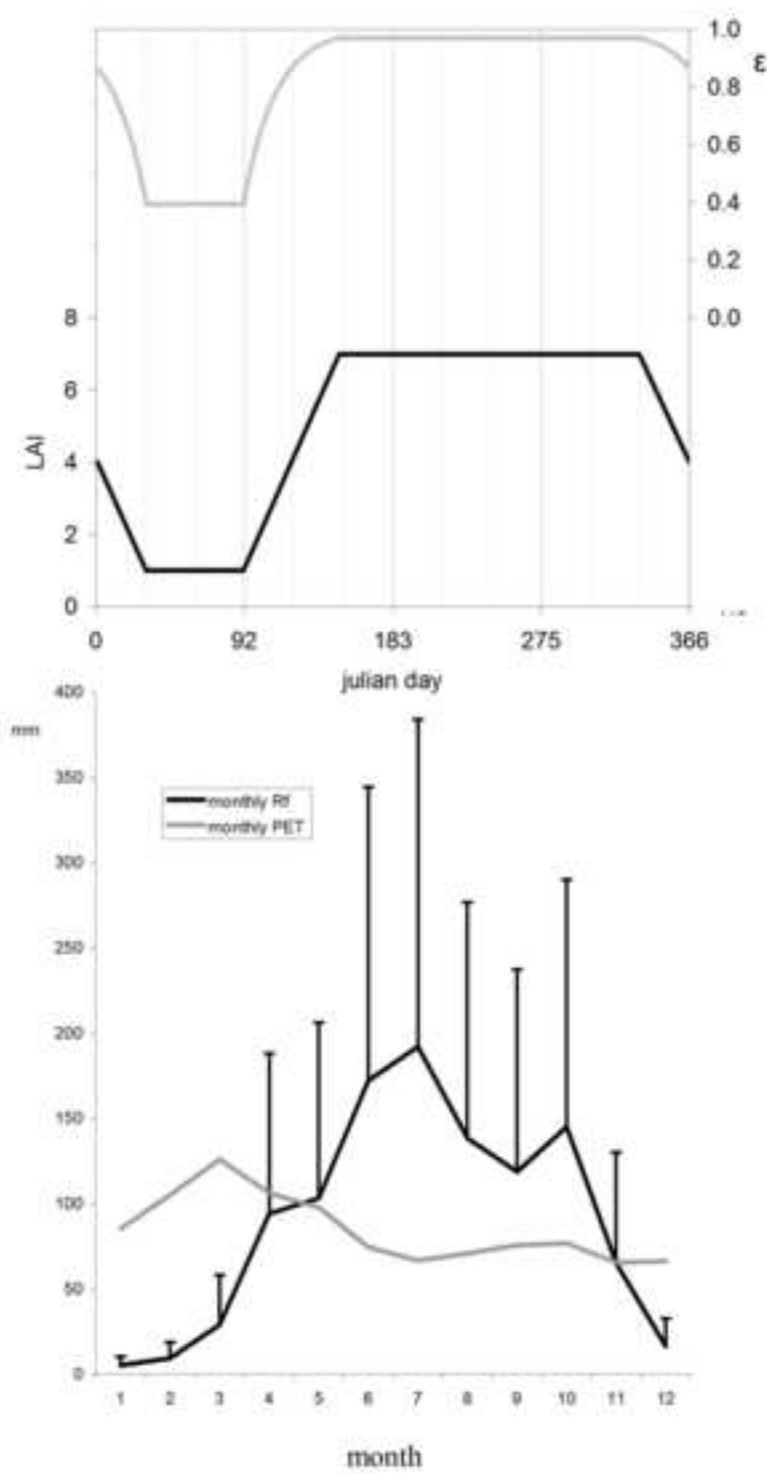


Figure 5
[Click here to download high resolution image](#)

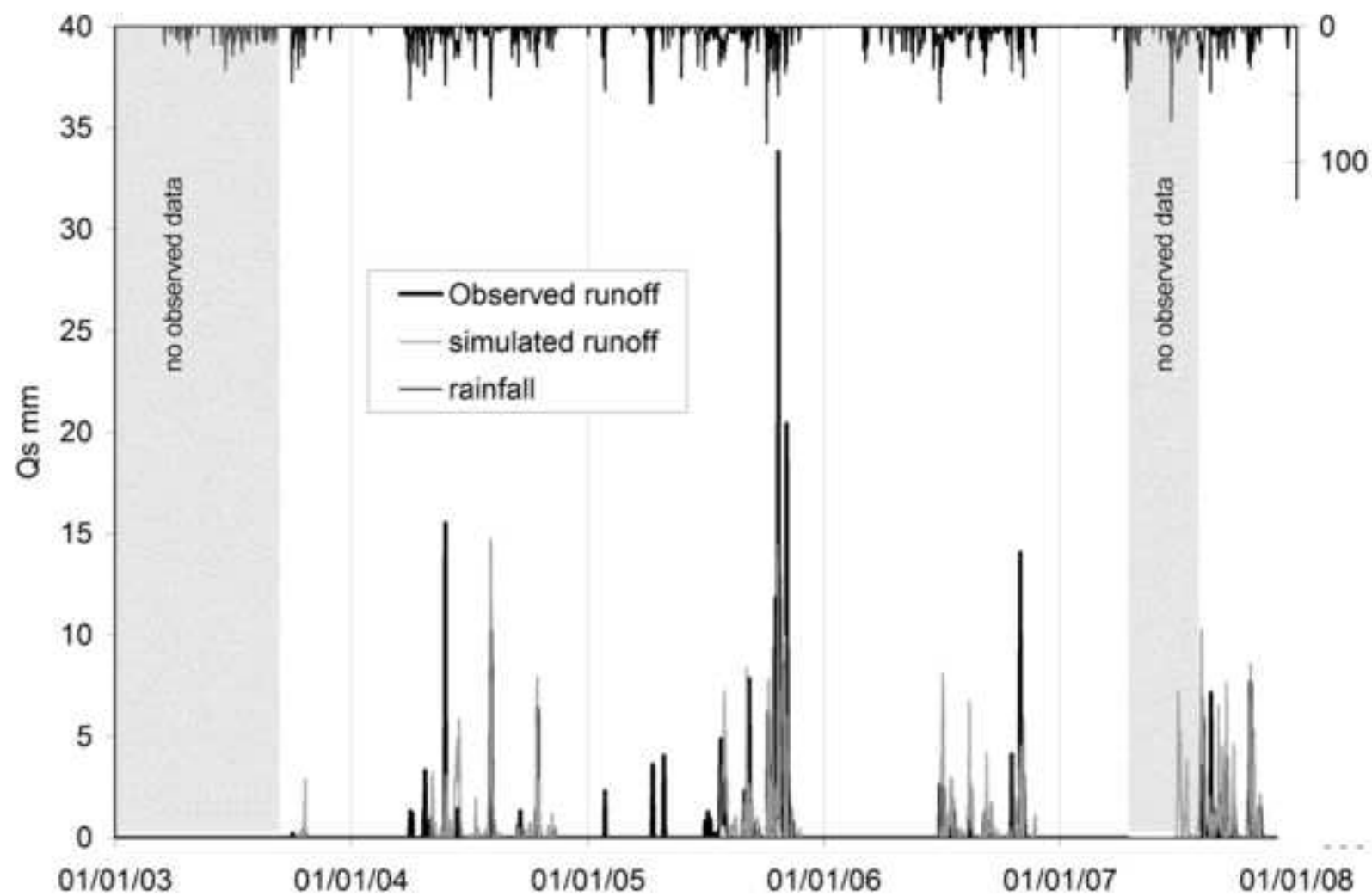


Figure 6
[Click here to download high resolution image](#)

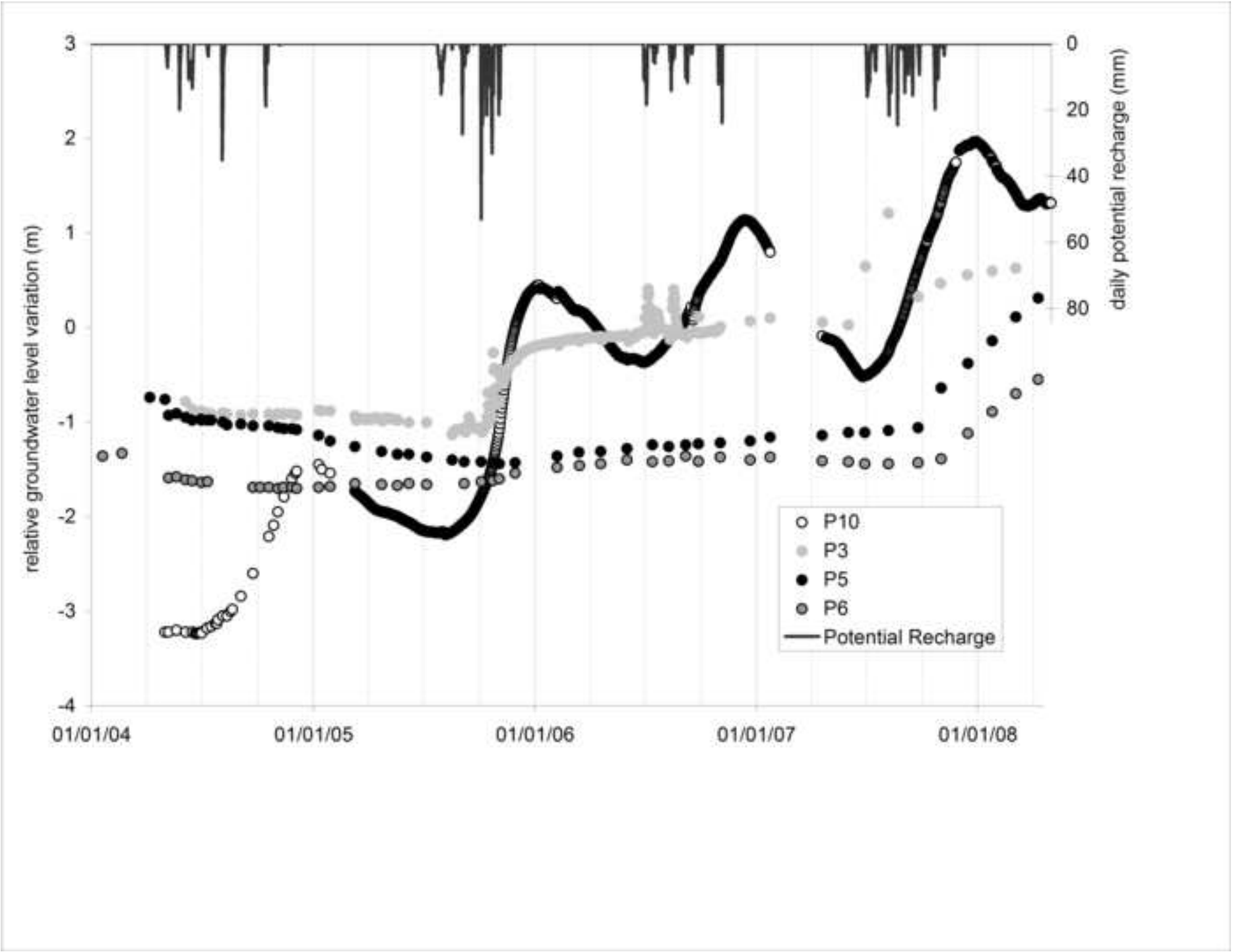


Figure 7
[Click here to download high resolution image](#)

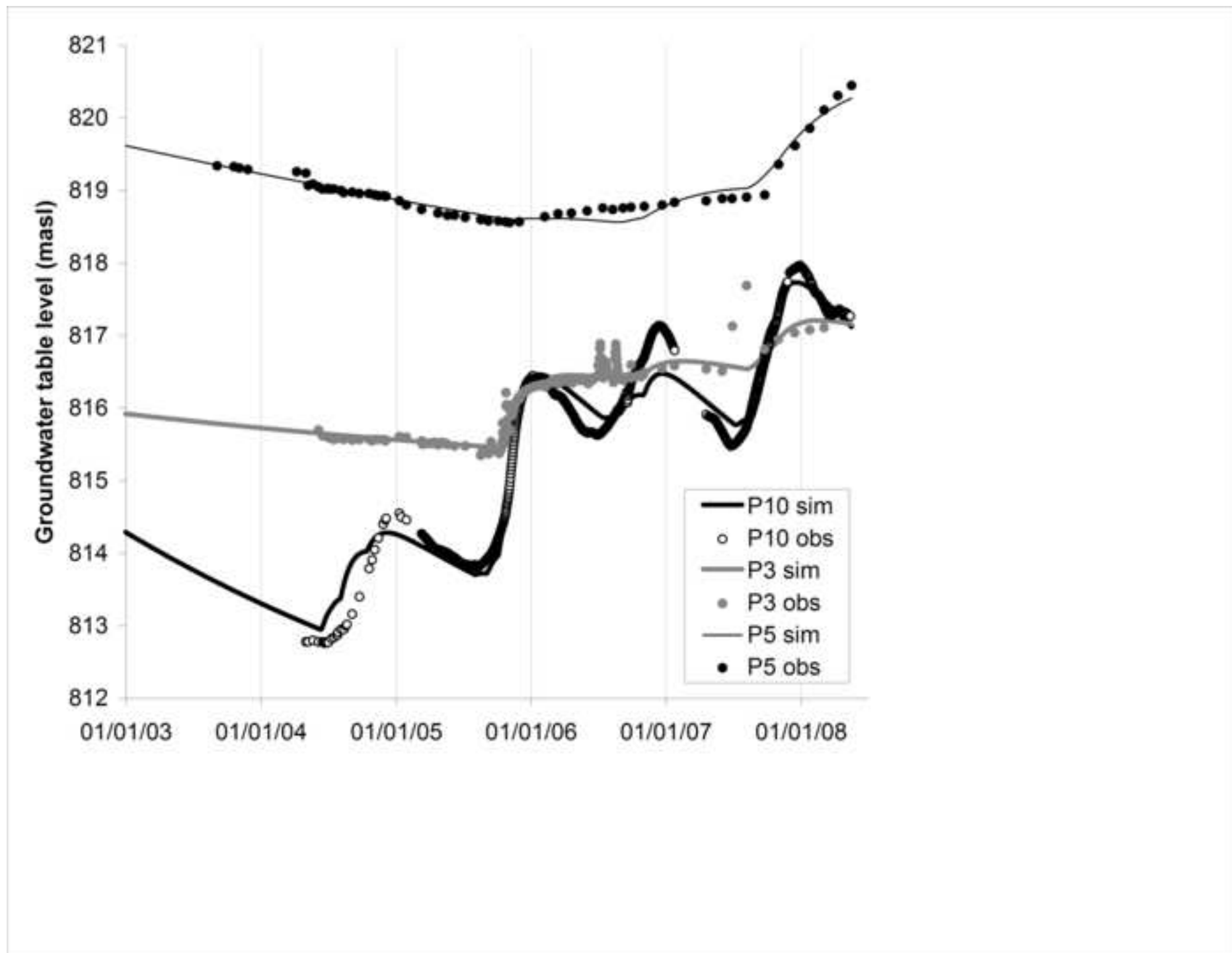


Figure 8
[Click here to download high resolution image](#)

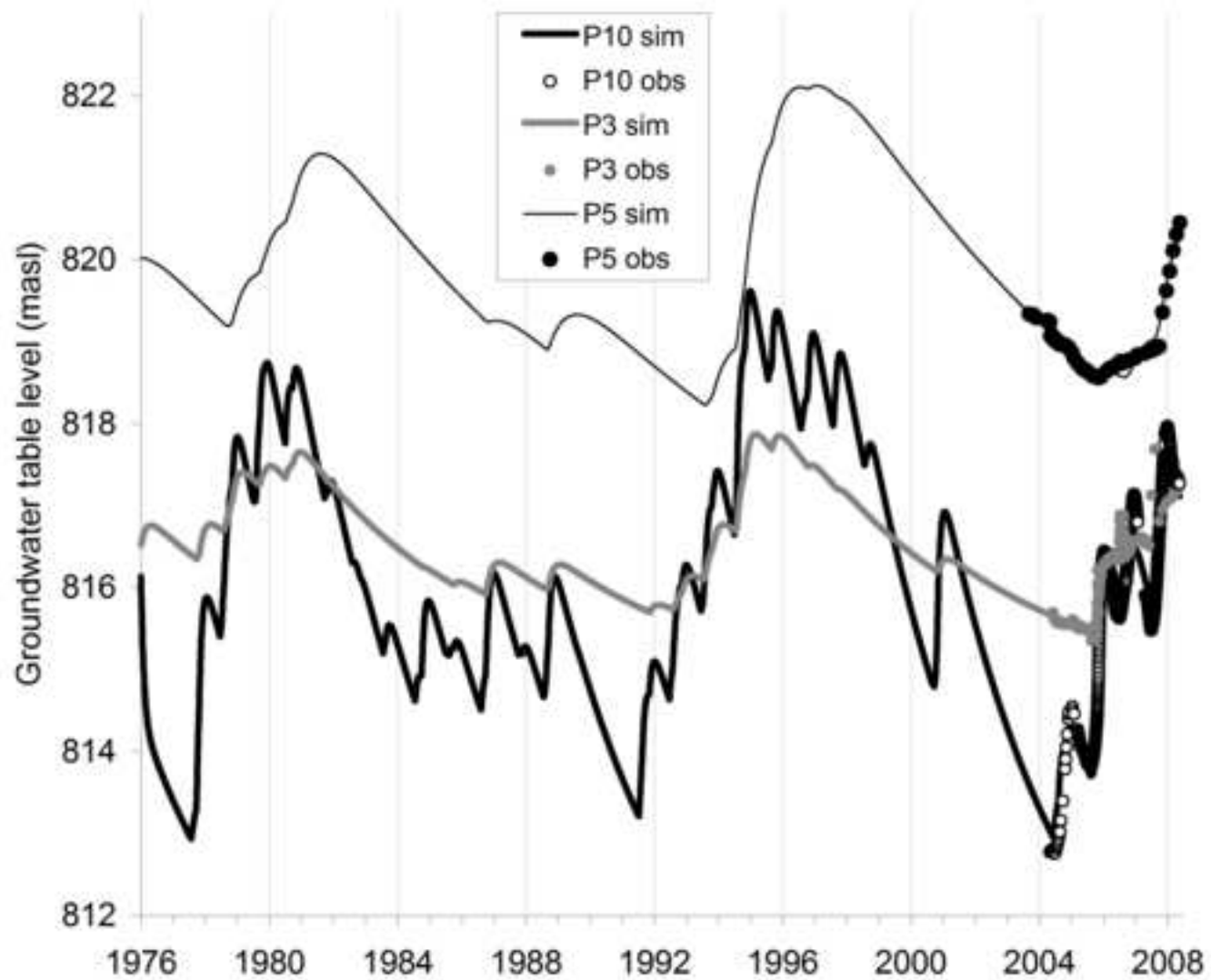


Figure 9
[Click here to download high resolution image](#)

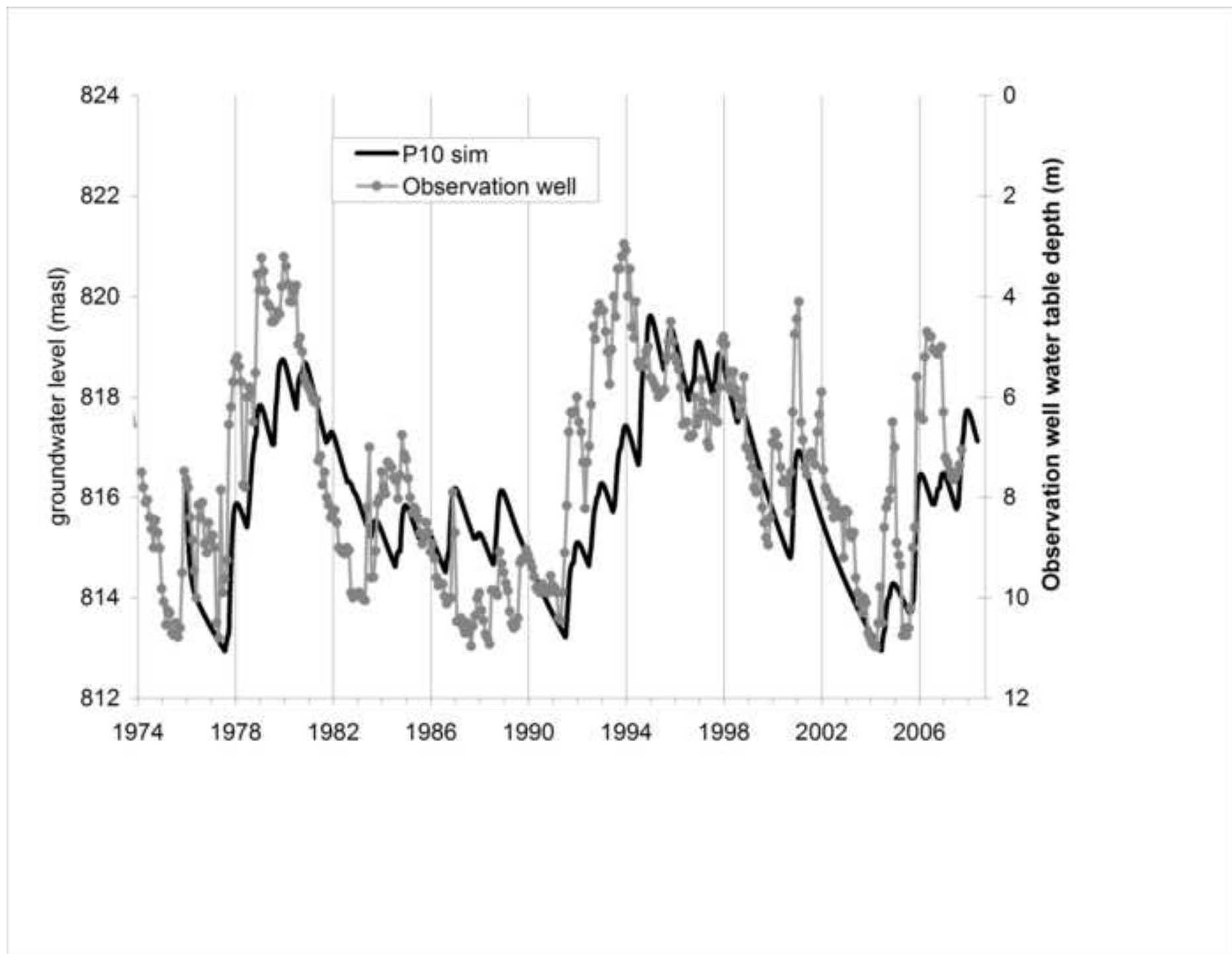
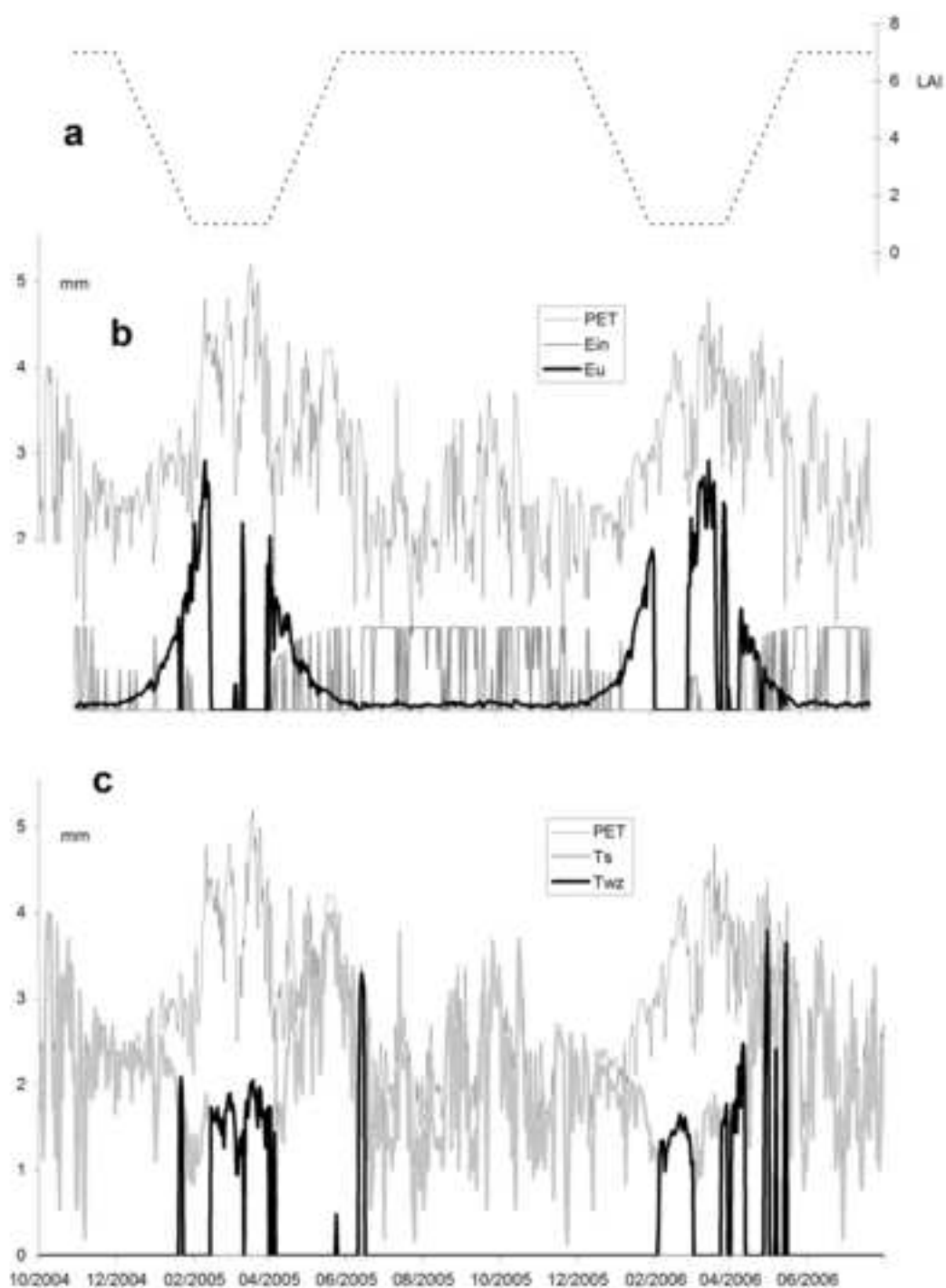


Figure 10
[Click here to download high resolution image](#)



	2003	2004	2005	2006	2007	2003-2007	cv %	1976-2007	cv %
Rf	706	1216	1434	1170	1252	1155	(23)	1091	(32)
PET	1101	1074	1017	1012	963	1034	(5)	1067	-
E_{in}	78	130	133	123	136	120	(20)	98	(23)
E_u	53	79	111	127	72	89	(34)	82	(33)
T_s	555	627	624	649	546	600	(8)	624	(11)
AET_s	686	837	868	900	754	809	(11)	803	(14)
PR	6	225	372	183	318	221	(64)	197	(87)
PET_{wz}	268	144	97	87	118	143	(51)	158	(58)
Obs Qs	1	66	196	52	-	79 *	(105)	-	-
sim Qs	5	117	154	92	162	93 *	(68)	94	(79)

Table 1 : Soil water balance (mm/year) for the monitored year and yearly average for the monitored period and the whole 32 year simulated period. Signification of terms is in the text.
*2003-2006 average

	P10	P3	P5
Ground level (masl)	832.82	844.24	859.14
initial watertable depth (m)	16.82	27.75	39.14
<i>parameters:</i>			
L ₀	809.93	814.73	814.85
WZMD _{max}	50	250	470
α ₁	6.96 10 ⁻⁴	4.89 10 ⁻⁴	2.32 10 ⁻⁴
Sy	2.10 10 ⁻³	6 10 ⁻³	5.11 10 ⁻³
α ₂	3.03 10 ⁻²	1.71 10 ⁻²	4.39 10 ⁻³

Table 2 : model parameters for the 3 simulated piezometers.

	2003-2007	cv %	1976-2007	cv %
Rf	1155	(23)	1091	(32)
AET_s	809	(11)	803	(14)
sim Qs	107	(59)	94	(79)
<i>Local balance</i>				
P10 T _{WZ}	31	(83)	43	(52)
P10 Q _{GW}	115	(28)	141	(26)
P3 T _{WZ}	62	(89)	114	(53)
P3 Q _{GW}	49	(38)	68	(35)
P5 T _{WZ}	62	(89)	141	(47)
P5 Q _{GW}	34	(8)	42	(22)
<i>Watershed balance</i>				
T_{WZ}	53	(88)	104	(43)
Q_{GW}	62	(23)	78	(26)
<i>water balance</i>	125	(103)	12	(1346)

Table 3: watershed balance components (in mm/year) for the piezometers P10, P3 and P5, for the monitoring period and the 31 year simulation and average watershed balance components.